Environmental Science Processes & Impacts

ROYAL SOCIETY OF CHEMISTRY

PAPER

View Article Online
View Journal | View Issue

Cite this: *Environ. Sci.: Processes Impacts*, 2026, **28**, 392

Brewing plastics: OCT reveals microplastic release from nylon tea bags in simulated brewed tea infusions

Pramoda Maheshi Jayasekara,†[ab] Praveen Abhishek,†[c] Bimsara Sandaruwan Kahandawala,†[bd] Nisala Damith,[e] Manura Weerasinghe,[c] Nipun Shantha Kahatapitiya,[e] Bhagya Nathali Silva,[bd] Shiromi Karunaratne,[f] Ruchire Eranga Wijesinghe,*[ab] Udaya Wijenayake,*[g] Anushka Upamali Rajapaksha *[c] and Meththika Vithanage[hc]

The release of microplastics (MPs) from nylon tea bags poses a critical concern for human exposure; however, their detection and quantification remain challenging especially in beverage matrices, and hence, this study pioneers the use of high-resolution optical coherence tomography (OCT) integrated with an image processing algorithm to rapidly detect and quantify the size and count of the MPs directly in the water extractions simulating tea brewing. The water extractions prepared by simulating tea brewing conditions, hot (100 °C, 1–5 min), cold (2 °C, 1 h), and ambient (30 °C, 1 h), were observed employing OCT imaging and validated through Nile Red (NR) staining and digital microscopy. The nylon tea bags steeped in hot water for 5 minutes released 16 000 to 24 000 LMPs (>30 μm) and SMPs (12–30 μm) per millilitre. The estimated daily intake (EDI) of MPs indicates a higher exposure for children (ranging from 0.201 to 0.349 $mm^3\ kg^{-1}\ day^{-1}$) compared to adults (0.046 to 0.080 $mm^3\ kg^{-1}\ day^{-1}$). In contrast, cold brewing for 1 hour released fewer LMPs but an equal quantity of small MPs (SMPs) compared to hot brewing. This OCT-based approach offers a rapid, versatile platform for the detection and quantification of MPs from diverse packaging materials and provides a powerful tool for comprehensive risk assessment when combined with chemical and toxicological analyses.

Received 18th August 2025
Accepted 15th November 2025

DOI: 10.1039/d5em00644a

rsc.li/espi

Environmental significance

The detection and quantification of microplastics (MPs) have become essential as MPs are now invading the food chain through plastic packaging. Here, we demonstrate the application of optical coherence tomography as a real-time, non-destructive, high-resolution imaging technology to detect MPs as small as 12 μm without any sample preprocessing such as filtration or staining. Optical coherence tomography (OCT) was applied to detect Large MPs (LMPs) (30–5 μm) and Small MPs (SMPs) (12–30 μm) MPs leached from nylon tea bags into tea infusions simulating real-world brewing conditions. Additionally, an integrated automated image-processing algorithm enabled volumetric quantification of MP count, volume, and length, enabling a more realistic and reproducible assessment than conventional methods. This approach positions OCT as a promising alternative for the volumetric evaluation of MPs in environmental samples, and its real-time, non-destructive nature enhances the efficiency of monitoring and assessment of MPs.

[a]*Department of Electrical and Electronic Engineering, Faculty of Engineering, Sri Lanka Institute of Information Technology, Malabe 10115, Sri Lanka. E-mail: eranga.w@sliit.lk*

[b]*Center for Excellence in Informatics, Electronics & Transmission (CIET), Sri Lanka Institute of Information Technology, Malabe 10115, Sri Lanka*

[c]*Ecosphere Resilience Research Centre, Faculty of Applied Sciences, University of Sri Jayewardenepura, Nugegoda 10250, Sri Lanka. E-mail: anurajapaksha@sjp.ac.lk*

[d]*Department of Information Technology, Faculty of Computing, Sri Lanka Institute of Information Technology, Malabe 10115, Sri Lanka*

[e]*School of Electronic and Electrical Engineering, College of IT Engineering, Kyungpook National University, 80, Daehak-ro, Buk-gu, Daegu 41566, Republic of Korea*

[f]*Department of Civil Engineering, Faculty of Engineering, Sri Lanka Institute of Information Technology, Malabe, 10115, Sri Lanka*

[g]*Department of Computer Engineering, Faculty of Engineering, University of Sri Jayewardenepura, Nugegoda 10250, Sri Lanka. E-mail: udayaw@sjp.ac.lk*

[h]*Geological Survey of Denmark and Greenland, Øster Voldgade 10, 1350 Copenhagen, Denmark*

† These authors contributed equally to this work.

1. Introduction

Plastic products are versatile and widely used in everyday life owing to their low cost, flexibility, durability, chemical stability, and lightness.[1] Global plastic production has increased from 1.5 million tons in 1958 (ref. 1) to 367 million tons in 2020.[2] It is estimated that it could reach up to three times higher by 2050.[3,4] Although plastic usage in food and beverage packages has risen due to the convenience and long shelf life they help to provide,[2] the extensive use of plastics increases exposure to microplastics (MPs) through food items.[5] Since MPs can be found in various food materials, such as beverages,[6] dairy products,[7] and bottled drinking water,[8] their ingestion leads to several health

implications, including tissue damage, fibrosis, inflammation and cytotoxicity,[1] which have not yet been documented descriptively.

Tea is one of the most widely consumed drinks, with an annual global production of 6.3 million tonnes,[9] and is frequently served in plastic (nylon) mesh bags, which have a high tendency to release a significant number of MPs, including small MPs (SMPs) (1–20 μm) and large MPs (LMPs) (20 μm to 5 mm) into beverages.[10] Notably, previous studies have documented that brewing a single plastic teabag at 95 °C releases billions of MPs and nano-plastics (NPs) into a single cup of tea.[11–14] Hence, the detection and identification of MPs in food matrices are critical for assessing their health risks. Although state-of-the-art methods, such as Fourier-transform infrared spectroscopy (FTIR),[2] Raman microscopy,[12] scanning electron microscopy (SEM),[15] optical microscopy,[6] spectral imaging[11] and fluorescence microscopy[9] have been employed effectively for polymer identification,[16] morphological analysis,[3] and fluorescence detection of polymeric compounds,[9,17] they are often limited by high cost, extensive sample preparation, high time consumption,[17,18] inaccurate quantification of particle count and size and poor detection of tiny particles (<20 μm), which highlights the need for a rapid, non-invasive, label-free, and high-resolution technique to detect and quantify MPs in complex matrices in real-time.

Optical coherence tomography (OCT) is a high-resolution, real-time, non-destructive biomedical imaging technology, which can be well implemented as a perfect candidate for the structural identification of LMPs and SMPs.[19] Although previous studies have used OCT to investigate internal structures of MP nurdles under extreme environmental conditions[20] and assess the MP deposition in fish gills,[21] these studies are limited to the internal structural observation and are yet to explore the real-time, volumetric analysis of MPs released from plastic consumer products. Unlike conventional methods, OCT is a label-free imaging technology which requires no extensive sample pre-processing, such as filtration and staining,[22] which positions it as a promising alternative to conventional MP detection techniques. Despite its potential, the utilisation of OCT for both the detection and accurate quantification of MPs, particularly when the particle count is exceptionally high (around 1×10^4), in different matrices, is yet to be explored.

This study integrated OCT with automated volumetric analysis, enabling high-throughput assessment of MP release, capturing the temporal and spatial variations of MPs induced by brewing conditions, such as temperature and steeping duration. Additionally, this unique integration enables highly detailed, real-time, non-destructive quantification of MPs, which is yet to be achieved *via* traditional microscopic and spectroscopic methods, which are mostly limited to static, endpoint measurements and often require labour-intensive sample preprocessing. This innovative approach offers a transformative methodological advancement, providing critical insight into exposure assessment and enabling rapid screening and risk evaluation of plastic consumer products. By enabling a more precise assessment of human exposure and environmental release pathways, this approach allows the establishment of regulations and mitigation strategies for plastic pollution in the food and beverage industry.

2. Materials and methods

2.1 Sample collection and preparation

Empty nylon tea bags (without tea leaves), intended for tea packaging, were selected and carefully rinsed with reverse osmosis (RO) water to eliminate any contaminants, following the methodologies established by previous studies.[2,23] The RO water was filtered through 1.2 μm pore size, 47 mm diameter Whatman GF/C glass microfibre (GE Healthcare Life Sciences) filter papers to remove contaminants. These steps were followed to enable the detection and quantification of MPs released from the nylon tea bags themselves, avoiding interference from tea leaves or the infusion dynamics that could complicate the detection. Each prepared nylon teabag was individually immersed in cleaned and sterilised glass containers containing 100 mL RO water at 100 °C. The tea bags were steeped for controlled durations of 1, 2, 3, 4, and 5 minutes. In addition to the effect of time on MP release, the influence of temperature was determined by steeping the tea bags at 2 °C and 30 °C for 1 hour, as extended cold brewing is a commonly adopted method for extracting bioactive compounds and enhancing the taste and aroma.[24,25] After each steeping, the tea bags were carefully removed, and the glass containers were immediately covered with aluminium foil and sealed with their caps to avoid contamination before further analysis. All sample preparations were performed wearing a cotton laboratory coat and gloves to prevent contamination.[6] The control sample was prepared using 100 mL of RO water without immersing a tea bag to identify the background contamination introduced through airborne fibres, equipment, or reagents, even under controlled conditions.[6]

2.2 Detection of microplastics using optical coherence tomography

A high-resolution swept-source OCT (SS-OCT) system (Model VEG210C1/M, Vega™ Series, Thorlabs Inc., USA) was used to scan the water extractions simulating tea brewing and investigate the released MPs. This SS-OCT system consists of a broadband swept-source laser with a central wavelength of 1300 nm and a sweep bandwidth of 110 nm. The axial resolution is 14 μm in air, while the lateral resolution is 20 μm in air. Volumetric scans were conducted over a field of view (FOV) measuring 1.6 cm × 1.6 cm × 0.828 cm, using a refractive index of 1.33 (for water). The water samples were thoroughly shaken to ensure a uniform distribution of MPs throughout the container.[20]

2.3 Identification of microplastics in samples using digital microscopic imaging and Nile red fluorescence

The water extractions simulating tea brewing were vacuum filtered using 1.2 μm pore size, 47 mm diameter Whatman GF/C glass microfibre filters (GE Healthcare Life Sciences) to collect the MPs.[1] The filter papers were examined by digital microscopy (Celestron Handheld Digital Microscope Pro, paired with Celestron Micro Capture Pro software) with 20× magnification to detect and observe MPs. The NR (9-diethylamino-5*H*-benzo[*a*]

phenoxazin-5-one) staining method was employed to quantify the MPs in the filter papers.[26] The NR solution was prepared by dissolving 0.01 g of NR dye in 1 L of absolute ethanol to create a 10 mg L^{-1} solution. Following the vacuum filtration of water extractions, three drops of the NR solution were gently added along the inner glass wall of the filter funnel to ensure uniform dye distribution on the filter paper. The dye was allowed to remain on the filter paper for 20 minutes. Subsequently, the filter papers were dried at 45 °C for 15 minutes, and any excess NR dye was rinsed off with RO water and dried again at 45 °C for another 15 minutes. Fluorescence imaging was performed using a 420–470 nm UV Crime-lite® 2 Blue light torch,[26] and the stained filter papers were photographed with a digital single-lens reflex (DSLR) camera (Canon EOS 250D DSLR (EFS 18–55 mm)) fitted with an orange camera lens filter (MACRO 0.25 m/0.8 ft) under low light conditions to identify the potential MPs (Fig. 1).[27] The Nile red-stained microplastics emitted yellow-orange fluorescence (~570–650 nm).

2.4 Algorithm for three-dimensional particle analysis

An automated data pipeline was developed to calculate the volume and length of each particle and cluster them based on their spatial position within the 3D volume. The algorithm consists of three main stages: pre-process, 3D binary mask generation by OCT images (binary volume construction), and 3D connected component analysis, followed by quantitative particle analysis. The scanned volumetric data were stored as 1200 images. Each 2D OCT image has a pixel resolution of 2504 × 976.

2.4.1 Pre-processing. Each OCT image underwent a standardised pre-processing procedure to achieve isotropic scaling consistent with the physical FOV of 16 × 16 mm before volumetric reconstruction, which was achieved by resampling the width of cross-sections (X-axis) from 2504–2400 pixels. Subsequently, the height of the cross-section (Y-axis) was proportionally rescaled to maintain the original aspect ratio. As a final step of the pre-processing phase, the number of cross sections was increased from 1200 to 2400 by sequentially duplicating each 2D-OCT image, resulting in a volumetric data grid of 2400 × 2400 × 935 ($H \times W \times N$) pixels.

2.4.2 3D binary mask generation. The stack of 2D-OCT images was converted into a binary 3D volume. First, the algorithm converted each grayscale 2D-OCT image $I_k(x, y)$ where $k = 1, 2, 3, \ldots, N$, into a binary image $b_k(x, y)$ using a fixed threshold T. This segmentation process is defined by using eqn (1).

$$b_k(x,\ y) = \begin{cases} 1 & \text{if } I_k(x,\ y) \geq T \\ 0 & \text{if } I_k(x,\ y) < T \end{cases} \quad (1)$$

where $b_k(x, y)$ represents the kth binary image and pixels classified as background are assigned 0 and foreground (MPs) pixels are assigned 1. All binary images were stacked along the depth dimension (Z-axis) to construct the 3D binary volume $B(x, y, z)$, which can be expressed using eqn (2), where $z = k$.

$$B(x,\ y,\ z) = \bigcup_{k=1}^{N} b_k(x,\ y) \quad (2)$$

This process generates a volumetric binary representation (eqn (3)).

$$B \in \{0, 1\}^{H \times W \times N} \quad (3)$$

2.4.3 3D connected component labelling. After the binary 3D mask generation process, the 3D mask undergoes a 3D connected component analysis (CCA) process. The algorithm applied 3D connected component labelling to B to isolate each particle (voxel cluster). Each voxel cluster C_i (component i) satisfies 26-connectivity. This process is expressed as eqn (4),

$$C_i = \{(x, y, z) \in B | \text{connected under 3D adjacency}\} \quad (4)$$

The algorithm computed the volumetric size, length, and the 3D coordinates of the centroid for each connected component C_i, using eqn (5), (6), (7) and (8), respectively.

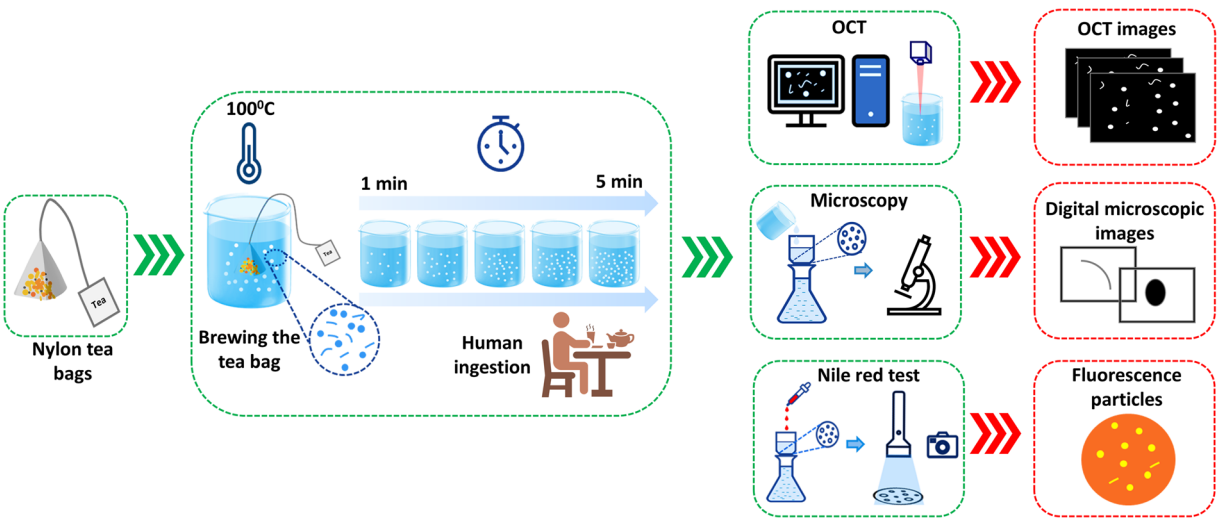

Fig. 1 Graphical overview of the experimental design illustrating the key steps and procedures.

Volume (voxel count),

$$V_i = |C_i| \tag{5}$$

Particle length,

$$d(p,\ q) = \sqrt{(x_p - x_q)^2 + (y_p - y_q)^2 + (z_p - z_q)^2}, \tag{6}$$

where p and q represent any two voxels, defined by their 3D coordinates, that belong to the same particle (voxel cluster) C_i, and $d(p, q)$ denotes the Euclidean distance between them.

$$L_i = \max_{p,q \in C_i} d(p, q) \tag{7}$$

Coordinate of the centroid,

$$O_i = \frac{1}{|C_i|} \sum_{(x,y,z) \in C_i} (x,\ y,\ z) \tag{8}$$

2.5 Human exposure to microplastics

The EDI of MPs through the consumption of nylon teabags was quantified to evaluate the exposure of two age groups, including children and adults, to MPs using the following equation (eqn (9)).[1]

$$\text{EDI } \left(\text{mm}^3\ \text{kg}^{-1}\ \text{day}^{-1}\right) \text{ or (particles per kg per day)} = \frac{C \times \text{DI} \times \text{EF} \times \text{ED}}{\text{BW} \times \text{AT}}, \tag{9}$$

where C is the concentration of MPs. Two scenarios were considered in the concentration; the first scenario is the number of particles per mL, and the second scenario is the volume of MPs ($\text{mm}^3\ \text{mL}^{-1}$). The considered parameters were DI: average daily intake of tea (200 mL), ED: exposure duration (year), EF: exposure frequency (day year^{-1}), AT: averaging time (days), and BW: body weight (kg), respectively. The average body weight of a child and adult was considered to be 16 kg and 70 kg, respectively.[3,28]

3. Results and discussion

3.1 Evaluation of microplastic release at different hot brewing durations

Optical coherence imaging, complemented by digital microscopy and NR staining-based validation, was employed to analyse the release of MPs from commercially available empty plastic tea bags during hot brewing. The samples steeped for 1, 2, 3, 4, and 5 minutes were compared with the unbrewed control sample. Steeped samples exhibit a substantial amount of MPs, ranging from approximately 16 000 to 24 000 MPs, indicating the susceptibility of nylon tea bags to release MPs during brewing, as nylon is a thermally sensitive material prone to hydrolysis when in direct contact with hot water.[23] The heat causes the breakdown of ester/amide bonds in the polymer and releases the MPs.[29] In addition, chain scission makes the material more brittle and prone to fragmentation, which is a strongly temperature-dependent process.[30] Therefore, MP release is intensified at temperatures above 40–60 °C,[29,31] and rapid breakdown occurs at temperatures above 95 °C.[23]

3.1.1 Time-resolved microplastic detection and structural assessment.

Representative OCT cross-sections, enface images from 4 different depths, and 3D volumetric images provided detailed morphological information and spatial distribution of MPs in the simulated water extractions. The bright blue colour particles in OCT cross-sections ((a–d) inset images) and enface images ((e–h) inset images) represent the MPs. And the enface images indicate the depth-wise distribution of the MPs. The volumetric images (inset image (i)) of the scanned volume demonstrate the prominent spatial distribution of the scattering particles. The red colour particles in the volumetric images correspond to the MPs (Fig. 2–4 and S1–S3).

The control sample exhibits minimal suspended MPs (Fig. 2(a–i) inset images). The cross sections of the control sample exhibited only 2 MP particles. The enface images indicated that those MPs were located at depths of 0.09 and 0.13 m. The measurements of these MP fragments were confirmed to be less than 1 mm, which can probably represent the background contamination introduced through atmospheric deposition, equipment, or reagents.[32,33] The volumetric image of the control sample confirmed the absence of detectable MPs, indicating that the RO water was free from impurities. This sample detected two MPs in digital microscope images, exhibiting fluorescence under UV light, indicating background contamination (Fig. 2(j-P1, P2 and k-P1, P2)). These observations suggest using filtered RO water as the medium does not interfere with MP detection and enhances the applicability of OCT to assess the release of MPs from a wide range of food and beverage packaging materials, beyond nylon tea bags. In addition, the utilisation of an aqueous medium minimises the interferences from the complex substrates and ensures reliable MP detection.[34]

In contrast to the control samples, all water extractions simulating tea brewing conditions contained small spherical and fragment-shaped MPs,[35] which were well visualised through cross-sectional images of the samples that were steeped for 1, 2, and 3 minutes (Fig. 3(a–h) inset images, S1(a–h) inset images and S2(a–h) inset images). In addition, elongated, cylindrical fibre-like structures were observed in the cross-sectional and enface images of samples steeped for 4 and 5 minutes (Fig. 4(a–h) inset images and S3(a–h) inset images).[35,36] Previous reports revealed that tea bags release mostly fibres, fragments, and spherical-shaped MPs into the tea.[3,6,36] Furthermore, our results suggested that the abundance of tiny, rounded MPs was comparatively higher than that of elongated fibre-like MPs. Similar to Liu *et al.* (2023), ellipse, oval, and rod shapes were identified as the most abundant fragments, while fibres were the least abundant in environmental samples.[35] This observation can be more favourable, since fibre-like MPs tend to entangle within the digestive system more than spherical-shaped MPs.[5] The MPs in most samples were primarily within the depth range of 0 to 5.54 mm.

Most fibre-like structures detected were less than or approximately 1 mm in length. However, MPs detected in the samples steeped for 4 and 5 minutes (Fig. 4 and S3) were substantially longer than those found in the 1, 2, and 3 minute samples (Fig. 3(a–h) inset images, S1(a–h) inset images and

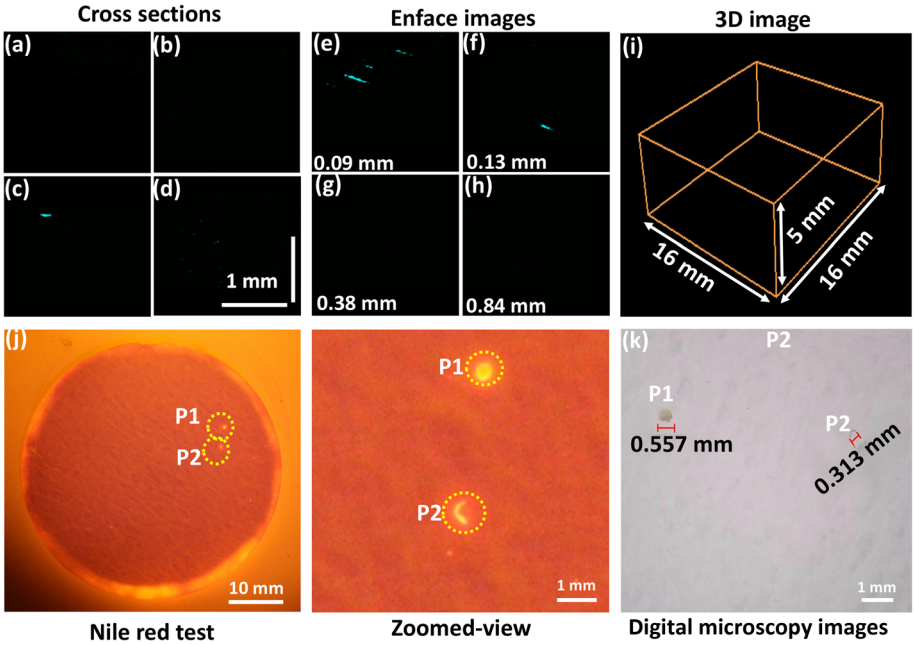

Fig. 2 Detection and visualisation of microplastics using optical coherence tomography, Nile red staining, and digital microscopic imaging in the control sample. ((a–d) inset images) Cross-sectional OCT images with representative microplastics. ((e–h) inset images) Enface OCT images with representative microplastics at 4 depth levels. (i) 3D visualisation of microplastics. (j) Sample after Nile red staining, indicating fluorescent microplastics at positions P1 and P2. The zoomed view shows clearer localisation of P1 and P2. (k) Digital microscope images: the microplastics corresponding to fluorescent particles.

S2(a–h) inset images), indicating an apparent increase in particle size with extended steeping. This trend indicated that longer steeping enhanced the release of larger MPs from nylon tea bags, similar to the prior studies.[37]

The volumetric image indicates that different-sized irregular-shaped MPs have been released into the water extractions during steeping (Fig. 2(i), 3(i), 4(i) and S1(i), S2(i), S3(i)). In addition, the increase in MP particle count can be identified

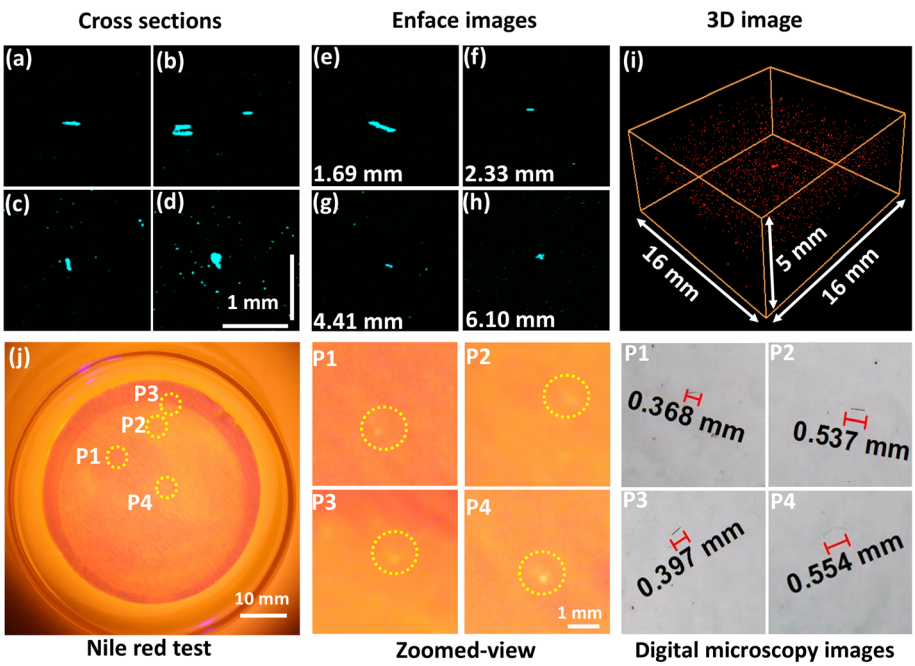

Fig. 3 Detection of microplastics using OCT, Nile red staining, and digital microscopic imaging after steeping the tea bag for 2 minutes. ((a–d) inset images) OCT cross-sections with representative microplastics. ((e–h) inset images) Enface OCT images at 4 depths. (i) 3D visualisation of microplastics. (j) Sample after Nile red staining, indicating representative fluorescent microplastics at positions P1, P2, P3 and P4. The zoomed view shows a more precise visualisation of P1, P2, P3, and P4 and digital microscope images for the microplastics corresponding to fluorescent particles.

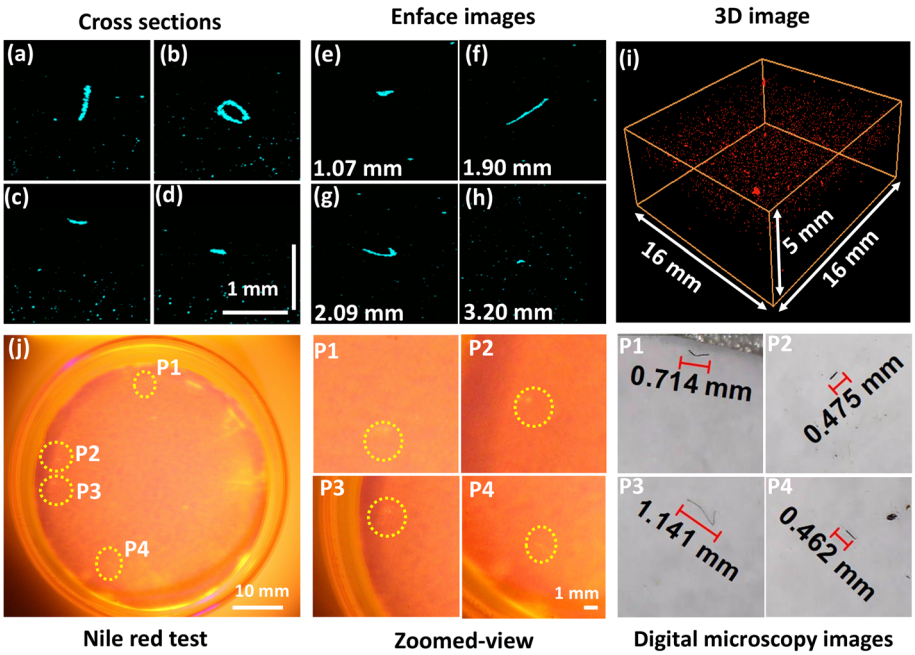

Fig. 4 Detection of microplastics using OCT, Nile red staining, and digital microscopic imaging after steeping the tea bag for 4 minutes. ((a–d) inset images) OCT cross-sections with representative microplastics. ((e–h) inset images) Enface OCT images at 4 depths. (i) 3D visualisation of microplastics. (j) Sample after Nile red staining, indicating representative fluorescent microplastics at positions P1, P2, P3 and P4. The zoomed view shows a more precise visualisation of P1, P2, P3, and P4 and digital microscope images for the microplastics corresponding to fluorescent particles.

when comparing the volumetric image of the sample steeped for 2 minutes with the sample steeped for 4 minutes. The numbers of MPs detected in the samples immersed for 1, 2, 3, 4, and 5 minutes by both NR staining and digital microscopic imaging were 8, 4, 7, 4, and 8, respectively (Fig. 2–4 and S1–S3(j-P1–P4)). The digital microscope images detected only the fragment and fibre-like MPs, which are larger than 0.3 mm, correlating with the OCT findings. Previous studies suggest that tea infusions contain MPs that fall within this size range, and the shape of the MPs is more similar to the MPs observed in this study.[2,38] Although NR fluorescence staining effectively highlighted fluorescent MPs, it detected fewer MPs than OCT, suggesting a potential underestimation of total MP presence. This discrepancy occurs due to tiny, stained particles that may remain invisible to the DSLR camera used for fluorescence imaging, despite successful fluorescence labelling.[4] Additionally, closely located or aggregated particles can be perceived as a single fluorescent particle, resulting in an underestimation of the particle count. Since this study mainly focused on MP detection and volumetric quantification, strictly controlled laboratory conditions were employed to reliably indicate that the particles detected by OCT originated from the nylon tea bags. Therefore, chemical compositional analysis was not performed, as the polymer type of the used tea bags was already known, and the primary focus of this study was on characterising the releasing behaviour and volumetric quantification of MPs.

In contrast, OCT examined the sample directly without filtration, thereby preventing aggregation and enabling the accurate three-dimensional detection of MPs. This highlighted the capability of OCT to visualise a larger quantity of MPs, possibly due to its ability to capture micrometre-level particles.

3.1.2 Quantitative analysis of microplastics during progressive brewing stages

3.1.2.1 Abundance of large microplastics and small microplastics. The abundance of MPs and their volume within the scanned volume (2 mL) were measured using the automated image processing algorithm applied to the OCT volumetric image. MPs larger than 30 μm were classified as LMPs, and those ranging from 12–30 μm were categorised as small MPs (SMPs)[10] (Fig. 5(a–d)). The scanned depth was divided into three depth levels: 0–2.77 mm (depth 1), 2.77–5.54 mm (depth 2), and 2.54–8.31 mm (depth 3), respectively. The abundance of LMPs demonstrates a steady increase, from 945–1600 LMPs over a steeping period of 1–5 minutes, suggesting that the release of LMPs increases with the extended steeping. The control sample exhibited 3 MPs. In addition, depth-wise analysis (Fig. 5(a and b)) indicates that most of the LMPs accumulate in the upper layer (depth 1) of all the samples. The abundance of LMPs at depth 1 varied from 386 to 697 MPs, while depths 2 and 3 exhibited 331 to 567 MPs and 228 to 358 MPs, respectively.

The abundance of SMPs is relatively high compared to that of LMPs. More than 90% of the MPs observed in the sample were SMPs (Fig. 5(b)), indicating that polymer degradation due to high temperatures caused the release of large quantities of SMPs, consistent with prior studies.[8,23] The sample steeped for 1 minute exhibits a high SMP abundance (18 769 MPs) compared to those immersed for 2, 3, and 4 minutes, suggesting the great

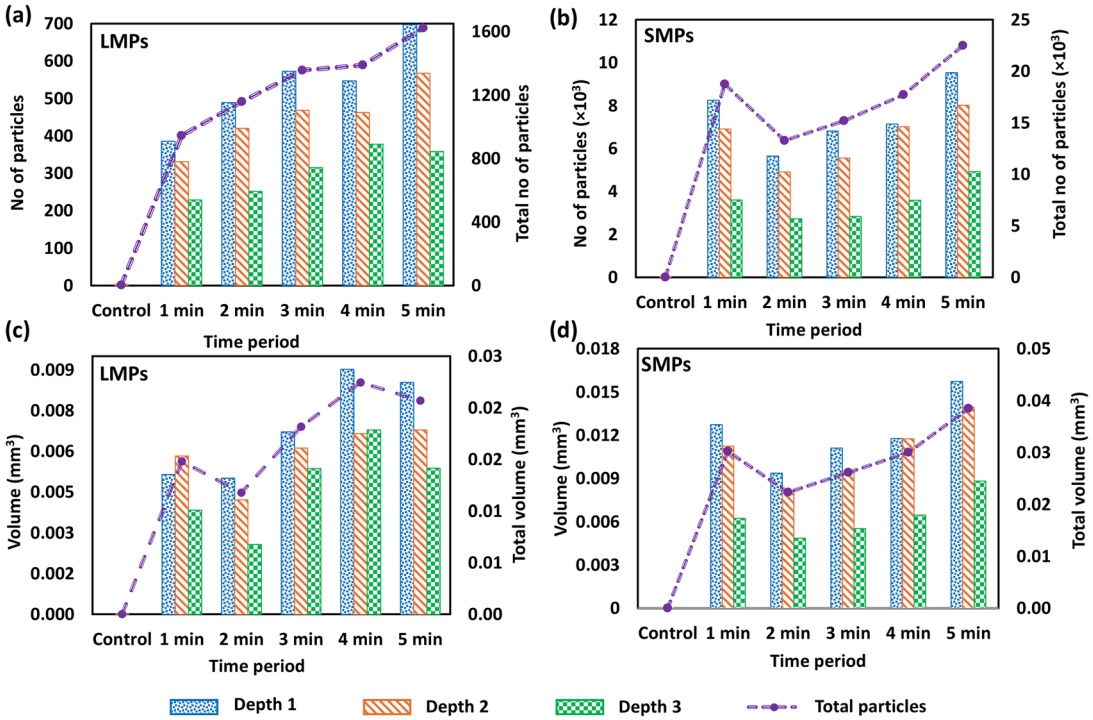

Fig. 5 Quantitative analysis of microplastics released from nylon tea bags over different steeping periods (1–5 minutes), categorised by 3 imaging depths. (a) Number of large microplastics detected at three imaging depths (depth 1 = 0–2.77 mm, depth 2 = 2.77–5.54 mm, and depth 3 = 5.54–8.31 mm) at each steeping interval. (b) Number of small microplastics detected at the same imaging depths at each steeping interval. (c) The volume of large microplastics at the same depths at each steeping interval. (d) The volume of small microplastics at the same depths at each steeping interval.

initial release of SMPs upon contact with hot water, as reported by Xu *et al.* (2021), who observed the rapid release of MPs from a single tea bag.[11] However, subsequent reduction of SMP count in other samples suggests that these SMPs have aggregated into larger particles. Samples steeped for 2, 3, 4, and 5 minutes illustrated a gradual increase in the number of SMPs from 13 273 to 22 489 MPs. Busse *et al.* (2020) clarified that 5800 to 20 400 SMPs can be released by one teabag during steeping for 5 minutes at 95 °C.[13] The depth-wise comparison of SMPs also suggests that most of the SMPs accumulate at depth 1, attributed to the buoyant nature of most plastic polymers, such as nylon and polypropylene, which have lower densities than water.[41]

3.1.2.2 Volume of microplastics. The total volume of LMPs varied from 0.011–0.022 mm^3, and SMPs varied from 0.022–0.038 mm^3. However, the total volume of LMPs and SMPs (Fig. 5(c and d)) exhibits a nonlinear trend. Even though the abundance of LMPs exhibited a steady increase in particle count, the highest total LMP volume among the samples was accumulated in the sample with a 4 minute steeping period (0.022 mm^3). The least total volume of LMPs was recorded in the control sample (7×10^{-6} mm^3), indicating low background contamination. The sample steeped for 1 minute exhibited a higher volume (0.015 mm^3) than the sample steeped for 2 minutes. The total LMP volume increased for the 2–4 minute steeped samples, indicating an increase in total MP volume over time. However, there is a slight decrease in the total LMP volume of the sample steeped for 5 minutes, suggesting that the release of large MPs into the tea tends to decrease beyond a certain duration (Fig. 5(c)). Although SMPs followed a comparable distribution trend, they did not significantly affect the overall volume of MPs detected in the 5 minute steeped sample. The total volume of SMPs in the sample steeped for 1 minute (0.030 mm^3) was higher than that of 2, 3, and 4 minutes. However, an increasing trend in the total volume of SMPs can be identified from 2–5 minute steeped samples. The highest SMP volume was recorded in the sample steeped for 5 minutes, and the lowest was recorded in the sample steeped for 2 minutes (Fig. 5(d)). To further understand the distribution, all the MPs were grouped into 4 volume ranges, and the number of MPs within each range was counted. According to Fig. S4, most MPs in each sample fall within the range of 5×10^{-7} to 1×10^{-6} mm^3, which was a size range that poses significant detection challenges for standard MP analytical methods. The least MPs were recorded in the volume greater than 5×10^{-5} mm^3.

3.1.2.3 Length fluctuations of microplastics. The MPs recorded in water extractions simulating tea brewing mainly vary from 12–702 μm (Fig. 6). LMPs were shown in the blue dotted scatter plots (Fig. 6(a–f)), while SMPs were represented in the green dotted scatter plots (Fig. 6(g–l)). Over the steeping durations, the length of MPs varied as follows: 30–437.28 μm at 1 minute, 30–373.85 μm at 2 minutes, 30–291.17 μm at 3 minutes, 30–702.35 μm at 4 minutes, and 30–437.30 μm at 5 minutes (Fig. 6(a–f)), respectively. The longest LMPs were recorded in the

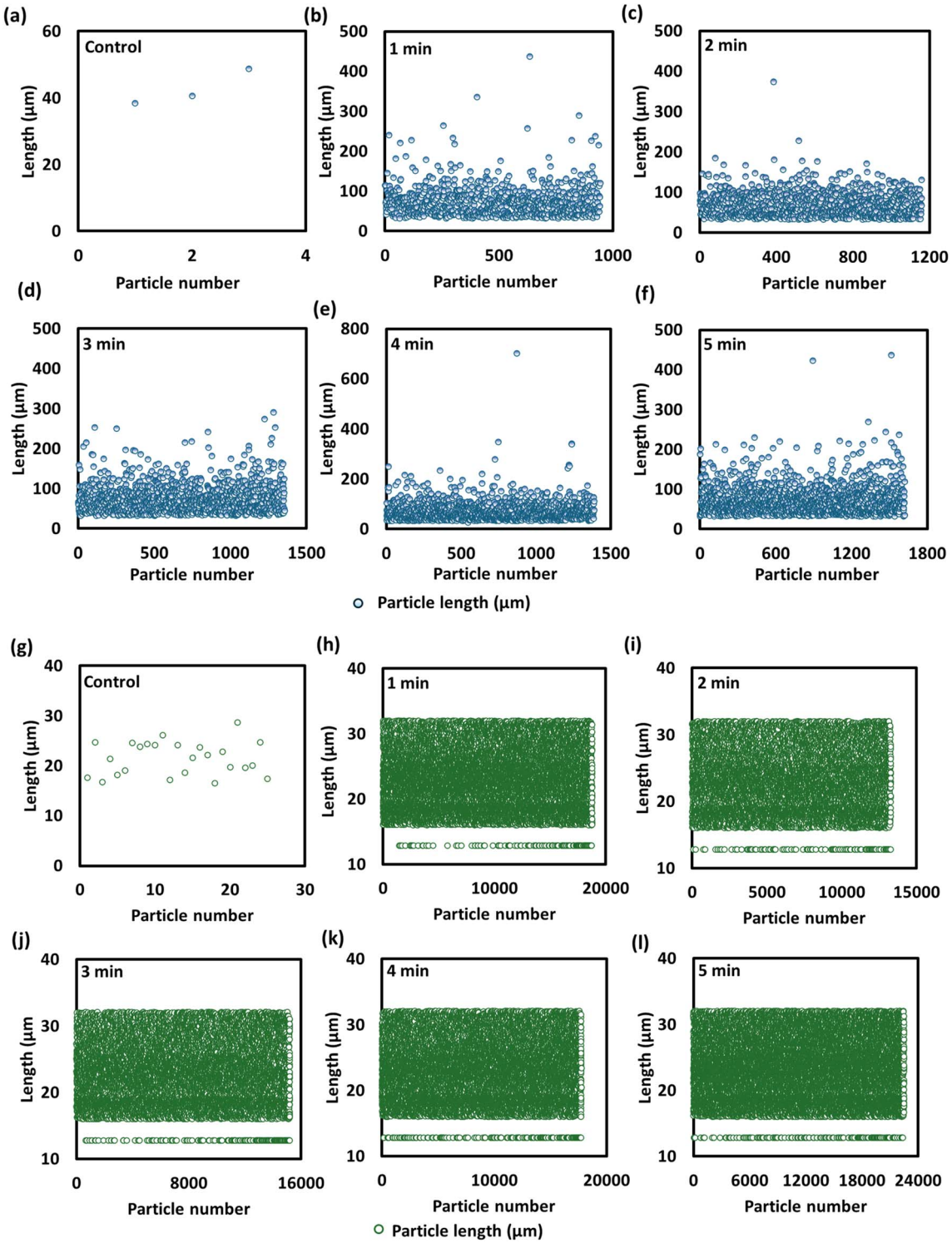

Fig. 6 Length distribution of the microplastics released from nylon tea bags during hot brewing. (a–f) The lengths of large microplastics and (g–l) the lengths of small microplastics. Each graph corresponds to brewing time (control sample (a and g) and 1 minute (b and h), 2 minute (c and i), 3 minute (d and j), 4 minute (e and k), and 5 minute (k and l)). Each dot represents the length of an individual MP particle.

sample steeped for 4 minutes. The SMPs in all samples exhibit lengths between 12 and 30 µm (Fig. 6(g–l)). Most prior studies, except for a few, have detected that the size of MPs released from tea bags into tea infusions varied within 100–2496 µm.[1,11,12,38] Notably, OCT revealed tiny MPs (12–100 µm), which were smaller than those in prior studies, highlighting the high sensitivity of OCT compared to traditional MP detection methods.[39,40]

3.2 Evaluation of microplastic release under cold and ambient brewing conditions

3.2.1 Temperature-dependent microplastic detection and structural assessment. At cold temperatures (2 °C), OCT cross sections and enface images visualised the fibre-like MPs and triangle-shaped MPs (Fig. S5).[35] In contrast, at 30 °C, OCT images revealed a predominance of small, irregular-shaped MP fragments (Fig. S6). Although both samples exhibited tiny, spherical-shaped MPs, the number of these MPs was higher in the samples steeped at 2 °C. In addition, the MPs visualised in the samples steeped at 2 °C were larger than those in the 30 °C sample (Fig. S5(e–h) and S6(e–h)), suggesting that cold temperatures also affect the release of larger MPs. Digital microscope images detected the MPs ranging from 0.72–2.46 mm in the sample steeped at 2 °C, while particles ranging from 0.13–1.04 mm were detected in the sample steeped at 30 °C. The MPs identified by the digital microscope in both samples exhibited fragment-like structures and a few fibre-like structures. Notably, 8 fluorescent particles were observed in both samples (Fig. S5(i) and S6(i)).

3.2.2 Quantitative analysis of microplastics during the cold and ambient brewing stages

3.2.2.1 Abundance of large microplastics and small microplastics. The results revealed that the MP particle count was higher for the sample steeped at 30 °C (1101 LMPs) than at 2 °C (462 LMPs). In contrast, the SMP count was higher at 2 °C (24 238 SMPs) than at 30 °C (21 705 SMPs). The samples steeped at low temperatures for 1 hour released fewer LMPs than those steeped at 100 °C, releasing numerous SMPs equal to those of hot brewing, as mentioned in prior studies.[37] This observation confirmed that the process of SMP release from tea bags depends not only on temperature. However, it took 1 hour to release this number of LMPs and SMPs into tea bags, indicating that the rate of MP release was lower under cold conditions (Fig. 7(a and b)). Prior studies also suggested that nylon releases MPs due to the hydrolysis of its amide bonds when exposed to water, even at low temperatures. Water penetrates the nylon and gradually breaks the polymer chains into tiny fragments.[42] Consistent with the hot brewing, most of the MPs accumulated in the upper layer of the sample, 200 LMPs at 2 °C and 481 LMPs at 30 °C. SMPs also followed the same pattern with 10 182 SMPs at 2 °C and 9524 SMPs at 30 °C, respectively.

3.2.2.2 Volume distribution of large microplastics and small microplastics. Notably, the volume of LMPs released from both samples exhibited similar MP volume (0.0078 mm^3). Compared to samples steeped at 100 °C, the volume of LMPs released during cold brewing was significantly lower, even though the sample was steeped for 1 hour. The volume of SMPs in the sample steeped at 2 °C was measured to be 0.028 mm^3, and that at 30 °C was 0.04 mm^3 (Fig. 7(c and d)). The total SMP volume of both samples was higher than that of LMPs. The number of MPs released during cold brewing indicates that most MPs fall within the volume range of 5×10^{-7} to 1×10^{-6} mm^3 (Fig. S7).

3.2.2.3 Length fluctuation of large microplastics and small microplastics. The sample remaining at 30 °C exhibited MPs ranging from 12–182 μm, and the sample at 2 °C exhibited MPs ranging from 12–1034 μm (Fig. 8). At 2 °C, only two MPs exceed 1 mm in length, while all the other MPs have lengths lower than

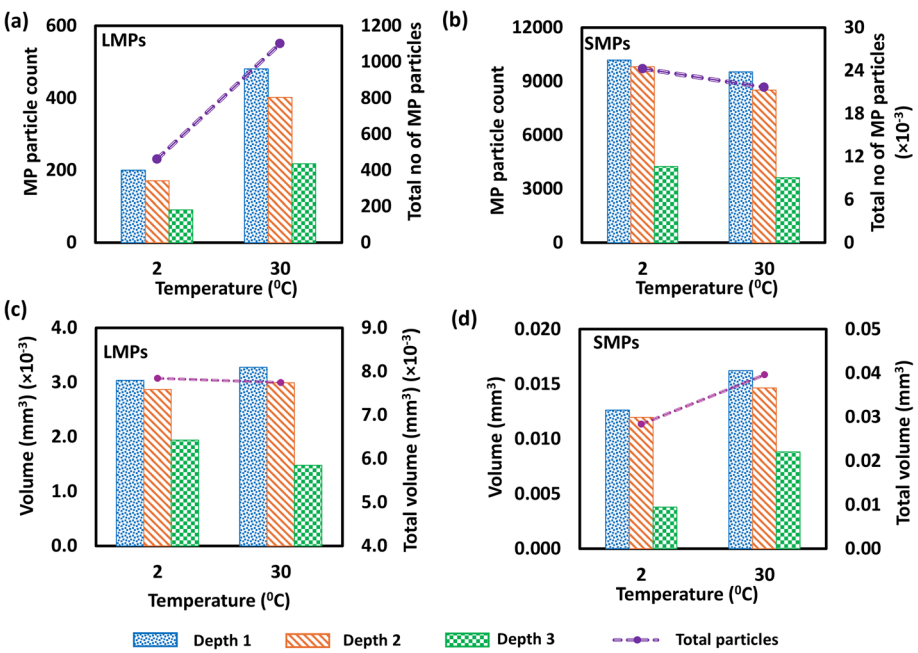

Fig. 7 Quantitative analysis of microplastics released from nylon tea bags over different steeping temperatures (2 °C and 30 °C), categorised by 3 imaging depths. (a) Number of large microplastics detected at three imaging depths (depth 1 = 0–2.77 mm, depth 2 = 2.77–5.54 mm, and depth 3 = 5.54–8.31 mm) at each steeping temperatures. (b) Number of small microplastics detected at the same imaging depths at each steeping temepratures. (c) The volume of large microplastics at the same depths at each steeping temperatures. (d) The volume of small microplastics at the same depths at each steeping temperatures.

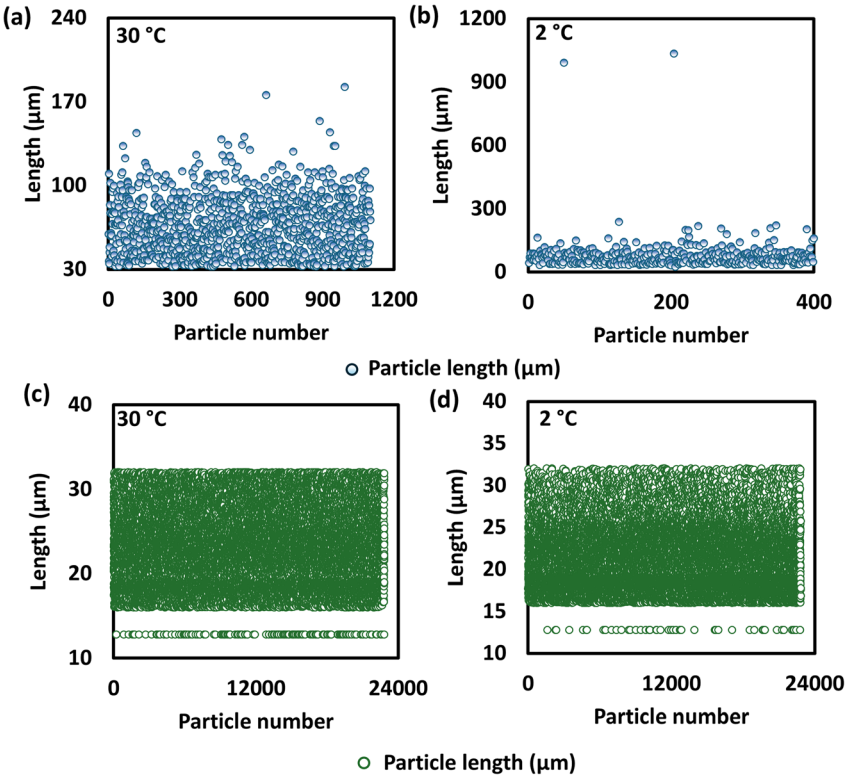

Fig. 8 Length distribution of microplastics released from nylon tea bags during cold brewing. (a and b) The lengths of large microplastics and (c and d) the lengths of small microplastics. Each column corresponds to brewing temperature (30 °C brewed sample (a and c) and 2 °C brewed sample (b and d)). Each dot represents the length of an individual particle.

Table 1 Microplastic concentration and estimated daily intake (EDI) for adults (70 kg) and children (16 kg) for drinking one cup of tea using nylon tea bags[a]

Brewing condition	Hot					Cold	Ambient
Time period	1 min	2 min	3 min	4 min	5 min	1 h	1 h
Temperature	100 °C	100 °C	100 °C	100 °C	100 °C	2 °C	30 °C
MP concentration (MP particles per mL)	9300.93	6862.36	7811.08	9027.78	11 440.88	10 983.73	11 641.85
MP concentration (volume (mm^3) per mL)	0.021	0.016	0.021	0.025	0.028	0.017	0.022
EDI – adult person (10^4) (particles per kg per day)	2.66	1.96	2.23	2.58	3.27	3.18	3.33
EDI – adult person (mm^3 kg^{-1} day^{-1})	0.061	0.046	0.060	0.071	0.080	0.05	0.06
EDI – child (10^5) (particles per kg per day)	1.163	0.858	0.976	1.128	1.430	1.373	1.455
EDI – child (mm^3 kg^{-1} day^{-1})	0.266	0.201	0.261	0.309	0.349	0.214	0.279

[a] EDI values were obtained with an assumption of one cup (200 mL) of tea consumed daily, with assumed body weights of an adult and a child being 70 kg and 16 kg, respectively. For hot-brewed samples, brewing temperatures were around 95–100 °C. For cold and ambient brewing, samples were kept at 2 °C and 30 °C, respectively, for 1 hour.

300 μm in both cold-immersed samples. This suggests that the cold conditions prominently release tiny MPs. Furthermore, it was confirmed that the low temperatures take an extended time to release the MPs, unlike hot brewing.[37]

3.3 Microplastic concentration and human exposure

The assessment of human exposure to MPs due to drinking tea is essential, since tea is one of the most popular beverages in the world.[1] The concentration and the EDI of the MPs reveal how different brewing conditions influence the potential oral ingestion of MPs. The concentration (MP particles per mL) exhibited an increasing trend (6862.36–11 440.88 MP particles per mL) (Table 1), indicating that prolonged steeping increases the release of MPs. It was noted that the particle count is relatively high, and the corresponding MP volume is low, ranging from 0.016 to 0.028 mm^3 mL^{-1}. This pattern indicated that the

released particles were small and followed the same pattern as the prior studies.[1,11,14]

The EDI values calculated based on particle count for adults and children were considerably higher compared to prior studies, particularly for children, due to their higher intake rate relative to body weight.[43] However, when MP exposure was evaluated based on volume, the EDI appeared much lower. This observation highlighted the importance of reporting both particle count and volume in human exposure assessments. As indicated in this study, relying solely on particle count led to an overestimation of exposure, particularly when a large proportion of the particles are SMPs. Therefore, a volume-based EDI assessment provided a more realistic evaluation, which conventional technologies cannot achieve.

The MPs were also detected in tea infusions prepared at 2 °C and 30 °C, with concentrations of 9083.73 MP particles per mL and 11 641.85 MP particles per mL, respectively, emphasising that both temperature and steeping duration influence the release of MPs.[37] The relatively high concentrations of MPs in tea infusions and EDI values highlight that the health risk associated with MP exposure cannot be ignored. Therefore, as a next step, integrating chemical characterisation and toxicological analysis with OCT-based analysis is necessary to accurately evaluate the potential health risk.[44] Additionally, the results suggest the importance of developing alternative materials to plastics[45] or an effective MP removal method. Prior studies have proposed several innovative approaches, including green starch–gelatin sponges[46] and oil-in-water emulsions,[47] which have high removal efficiencies in various food and environmental samples.

4. Conclusion

Microplastics are one of the pressing pollutants due to their ubiquitous nature. The discovery of MPs in food and beverages raised global concern regarding human exposure. As tea is one of the most frequently consumed beverages, this study was initiated to assess the release of MPs from nylon tea bags, a material widely used in the production of tea bags, particularly for herbal teas. This study successfully visualised and quantified the MPs released from tea bags in the 12–702 μm range using OCT as a cutting-edge, non-invasive, high-resolution, label-free, *in situ* imaging technique, overcoming the detection limitations of conventional methods. The NR staining and digital microscopic observation further validated the presence of MPs. An automated image processing algorithm allowed for the rapid quantification of particle count, volume, and length more efficiently. The tea bags released 6862.36–11 440.88 MP particles per mL during hot brewing for 1–5 minutes. The concentration of MPs based on the volume of MPs ranges from 0.016–0.025 $mm^3\ mL^{-1}$. The MP count increased over time (945–1622 particles), and SMPs exhibited an increasing trend after 2 minute steeped samples. The EDI of MPs ranged from 1.96×10^4 to 3.27×10^4 particles per kg per day and 0.046–0.080 $mm^3\ kg^{-1}\ day^{-1}$. The EDI was significantly higher for children, ranging from 85 779–143 011 particles per kg per day and 0.201–0.349 $mm^3\ kg^{-1}\ day^{-1}$. These findings were made possible by integrating OCT with an automated image processing algorithm for detecting and quantifying MPs. Thus, this integration represents a paradigm shift in MP analysis, offering a high-throughput alternative to more labour-intensive and time-consuming techniques. Furthermore, the OCT-based analysis can be extended to analyse MPs released from various tea bag materials and a wide range of food and beverage packaging materials and can be integrated with chemical characterisation and toxicological assays to support toxicological risk assessment.

Conflicts of interest

There are no conflicts to declare.

Data availability

The data supporting this study have been included in the main text or the supplementary information (SI). Supplementary information is available. See DOI: https://doi.org/10.1039/d5em00644a.

Acknowledgements

This work was supported by the National Science Foundation of Sri Lanka (Grant No. RG/2025/BS/13), a research grant funded by the University of Sri Jayewardenepura, Sri Lanka (Grant No. ASP/01/RE/ENG/2022/86) and research grants funded by the Sri Lanka Institute of Information Technology, Sri Lanka (Grant No. PVC(R&I)RG/2025/15 and PVC(R&I)RG/2025/28).

References

1 F. S. Kashfi, A. Mohammadi, F. Rostami, A. Savari, G. E. De-la-Torre, J. Spitz, R. Saeedi, M. Kalantarhormozi, A. Farhadi and S. Dobaradaran, Microplastics and phthalate esters release from teabags into tea drink: occurrence, human exposure, and health risks, *Environ. Sci. Pollut. Res.*, 2023, **30**, 104209–104222.

2 Ş. Güzel İzmirli and A. Gökkaya, Microplastic Pollution and Risk Assessment in Packaged Teas in Türkiye, *Water, Air, Soil Pollut.*, 2024, **235**, 438.

3 M. Ahmad, J. Ahmad, M. Usama, H. A. Al-Swadi, M. A. Mousa, M. I. Rafique, M. I. Al-Wabel and A. S. F. Al-Farraj, Microplastic contamination in commercial food and drink products and associated risk of potential human intake in Riyadh, Saudi Arabia, *Environ. Monit. Assess.*, 2025, **197**, 246.

4 A. Altunışık, Prevalence of microplastics in commercially sold soft drinks and human risk assessment, *J. Environ. Manage.*, 2023, **336**, 117720.

5 M. M. Joseph, J. B. Nair and A. M. Joseph, Microscopic menace: exploring the link between microplastics and cancer pathogenesis, *Environ. Sci.: Processes Impacts*, 2025, **27**, 1768–1795.

6 Y. Li, L. Peng, J. Fu, X. Dai and G. Wang, A microscopic survey on microplastics in beverages: the case of beer, mineral water and tea, *Analyst*, 2022, **147**, 1099–1105.
7 P. A. Da Costa Filho, D. Andrey, B. Eriksen, R. P. Peixoto, B. M. Carreres, M. E. Ambühl, J. B. Descarrega, S. Dubascoux, P. Zbinden, A. Panchaud and E. Poitevin, Detection and characterization of small-sized microplastics (≥ 5 μm) in milk products, *Sci. Rep.*, 2021, **11**, 24046.
8 D. Schymanski, C. Goldbeck, H.-U. Humpf and P. Fürst, Analysis of microplastics in water by micro-Raman spectroscopy: Release of plastic particles from different packaging into mineral water, *Water Res.*, 2018, **129**, 154–162.
9 N. J. H. Fard, F. Jahedi and A. Turner, Microplastics and nanoplastics in tea: Sources, characteristics and potential impacts, *Food Chem.*, 2025, **466**, 142111.
10 F. Du, The missing small microplastics: easily generated from weathered plastic pieces in labs but hardly detected in natural environments, *Environ. Sci.: Adv.*, 2024, **3**(2), 227–238.
11 J.-L. Xu, X. Lin, S. Hugelier, A. Herrero-Langreo and A. A. Gowen, Spectral imaging for characterization and detection of plastic substances in branded teabags, *J. Hazard. Mater.*, 2021, **418**, 126328.
12 T. Mei, J. Wang, X. Xiao, J. Lv, Q. Li, H. Dai, X. Liu and F. Pi, Identification and Evaluation of Microplastics from Tea Filter Bags Based on Raman Imaging, *Foods*, 2022, **11**, 2871.
13 K. Busse, I. Ebner, H.-U. Humpf, N. Ivleva, A. Kaeppler, B. E. Oßmann and D. Schymanski, Comment on "Plastic Teabags Release Billions of Microparticles and Nanoparticles into Tea", *Environ. Sci. Technol.*, 2020, **54**, 14134–14135.
14 G. Banaei, D. Abass, A. Tavakolpournegari, J. Martín-Pérez, J. Gutiérrez, G. Peng, T. Reemtsma, R. Marcos, A. Hernández and A. García-Rodríguez, Teabag-derived micro/nanoplastics (true-to-life MNPLs) as a surrogate for real-life exposure scenarios, *Chemosphere*, 2024, **368**, 143736.
15 R. Joshi, S. Adhikari, Y. Kim, D. Lee and B.-K. Cho, A qualitative method for detecting microplastics in liquid herbal medicine using gold nanoparticle SERS substrates, *J. Environ. Chem. Eng.*, 2025, **13**, 116006.
16 Q. Zhang, X. Wang, Y. Chen, G. Song, H. Zhang, K. Huang, Y. Luo and N. Cheng, Discovery and solution for microplastics: New risk carriers in food, *Food Chem.*, 2025, **471**, 142784.
17 A. Baruah, A. Sharma, S. Sharma and R. Nagraik, An insight into different microplastic detection methods, *Int. J. Environ. Sci. Technol.*, 2022, **19**, 5721–5730.
18 T. Stanton, M. Johnson, P. Nathanail, R. L. Gomes, T. Needham and A. Burson, Exploring the Efficacy of Nile Red in Microplastic Quantification: A Costaining Approach, *Environ. Sci. Technol. Lett.*, 2019, **6**, 606–611.
19 R. E. Wijesinghe, K. Park, Y. Jung, P. Kim, M. Jeon and J. Kim, Industrial resin inspection for display production using automated fluid-inspection based on multimodal optical detection techniques, *Opt Laser. Eng.*, 2017, **96**, 75–82.
20 P. M. Jayasekara, P. Abhishek, N. S. Kahatapitiya, M. Weerasinghe, B. S. Kahandawala, B. N. Silva, U. Wijenayake, A. U. Rajapaksha, R. E. Wijesinghe and M. Vithanage, Environmental forensics of the X-press pearl disaster: Uncovering the internal micro-structural transformations in marine microplastics, *J. Hazard. Mater.*, 2025, **496**, 139231.
21 P. C. Asani, Z. Alam and R. Poddar, Exploring the impact of PVC and PVA microplastics on zebrafish tissue using multi-spectral imaging, Optical Coherence Tomography (OCT) and biospeckle OCT (bOCT), *Chemosphere*, 2023, **341**, 140088.
22 D. Kalupahana, N. S. Kahatapitiya, D. Kamalathasan, R. E. Wijesinghe, B. N. Silva and U. Wijenayake, State-of-the-Art of Deep Learning in Multidisciplinary Optical Coherence Tomography Applications, *IEEE Access*, 2024, **12**, 164462–164490.
23 L. M. Hernandez, E. G. Xu, H. C. E. Larsson, R. Tahara, V. B. Maisuria and N. Tufenkji, Plastic Teabags Release Billions of Microparticles and Nanoparticles into Tea, *Environ. Sci. Technol.*, 2019, **53**, 12300–12310.
24 M. Muller, D. De Beer, C. Truzzi, A. Annibaldi, P. Carloni, F. Girolametti, E. Damiani and E. Joubert, Cold brewing of rooibos tea affects its sensory profile and physicochemical properties compared to regular hot, and boiled brewing, *LWT–Food Sci. Technol.*, 2020, **132**, 109919.
25 S. Uzuner and G. A. Evrendilek, Functional responses of cold brewed white tea to high pressure processing, *J. Food Process Eng.*, 2019, **42**(5), DOI: 10.1111/jfpe.13098.
26 D. Ho, S. Liu, H. Wei and K. G. Karthikeyan, The glowing potential of Nile red for microplastics Identification: Science and mechanism of fluorescence staining, *Microchem. J.*, 2024, **197**, 109708.
27 J. C. Prata, I. F. Sequeira, S. S. Monteiro, A. L. P. Silva, J. P. Da Costa, P. Dias-Pereira, A. J. S. Fernandes, F. M. Da Costa, A. C. Duarte and T. Rocha-Santos, Preparation of biological samples for microplastic identification by Nile Red, *Sci. Total Environ.*, 2021, **783**, 147065.
28 A. Yousefi, H. M. Attar and Z. Yousefi, Investigating the release of microplastics from tea bags into tea drinks and human exposure assessment, *Environmental Health Engineering and Management*, 2024, **11**, 337–347.
29 V. Kumar and P. Verma, Unveiling the hidden threat of microplastic in paper cups and tea bags: a critical review of their exacerbation and alarming concern in India, *Discover Appl. Sci.*, 2025, **7**(6), 527.
30 V. Caponigro, C. Di Fiore, F. Carriera, A. Iannone, A. Malinconico, P. Campiglia, C. Crescenzi and P. Avino, Evaluating microplastic emission from takeaway containers: A Micro-Raman approach across diverse exposure scenarios, *Food Chem.*, 2025, **464**, 141716.
31 T. Ali, A. Habib, F. Muskan, S. Mumtaz and R. Shams, Health risks posed by microplastics in tea bags: microplastic pollution – a truly global problem, *Int. J. Surg.*, 2023, **109**, 515–516.
32 K. Munno, A. L. Lusher, E. C. Minor, A. Gray, K. Ho, J. Hankett, C.-F. T Lee, S. Primpke, R. E. McNeish, C. S. Wong and C. Rochman, Patterns of microparticles in

blank samples: A study to inform best practices for microplastic analysis, *Chemosphere*, 2023, **333**, 138883.
33 E. Visentin, G. Niero, F. Benetti, C. O'Donnell and M. De Marchi, Assessing microplastic contamination in milk and dairy products, *npj Science of Food*, 2025, **9**(1), 135.
34 G. Erni-Cassola, M. I. Gibson, R. C. Thompson and J. A. Christie-Oleza, Lost, but Found with Nile Red: A Novel Method for Detecting and Quantifying Small Microplastics (1 mm to 20 μm) in Environmental Samples, *Environ. Sci. Technol.*, 2017, **51**, 13641–13648.
35 F. Liu, L. A. Rasmussen, N. D. R. Klemmensen, G. Zhao, R. Nielsen, A. Vianello, S. Rist and J. Vollertsen, Shapes of Hyperspectral Imaged Microplastics, *Environ. Sci. Technol.*, 2023, **57**, 12431–12441.
36 A. Soudavari, F. Barari, E. Ehsani, Z. Bonyadi and M. Davoudi, Occurrence and health risk assessment of microplastics in beverages and ice packs, *Sci. Rep.*, 2025, **15**(1), 23584.
37 A. A. Yaroslavov, A. A. Efimova, T. E. Grokhovskaya, A. G. Badikova, V. V. Spiridonov, D. V. Pozdyshev, S. V. Lyulin and J. M. Kenny, Evolution of Microplastics Released from Tea Bags into Water, *Polymers*, 2025, **17**, 2700.
38 V. C. Shruti, F. Pérez-Guevara, I. Elizalde-Martínez and G. Kutralam-Muniasamy, First study of its kind on the microplastic contamination of soft drinks, cold tea and energy drinks - Future research and environmental considerations, *Sci. Total Environ.*, 2020, **726**, 138580.
39 J.-L. Xu, K. V. Thomas, Z. Luo and A. A. Gowen, FTIR and Raman imaging for microplastics analysis: State of the art, challenges and prospects, *TrAC, Trends Anal. Chem.*, 2019, **119**, 115629.
40 A. M. Elert, R. Becker, E. Duemichen, P. Eisentraut, J. Falkenhagen, H. Sturm and U. Braun, Comparison of different methods for MP detection: What can we learn from them, and why asking the right question before measurements matters?, *Environ. Pollut.*, 2017, **231**, 1256–1264.
41 I. Chubarenko, Physical processes behind interactions of microplastic particles with natural ice, *Environ. Res. Commun.*, 2022, **4**, 012001.
42 A. D. Banjo, V. Agrawal, M. L. Auad and A.-D. N. Celestine, Moisture-induced changes in the mechanical behavior of 3D printed polymers, *Compos., Part C: Open Access*, 2022, **7**, 100243.
43 N. H. Mohamed Nor, M. Kooi, N. J. Diepens and A. A. Koelmans, Lifetime Accumulation of Microplastic in Children and Adults, *Environ. Sci. Technol.*, 2021, **55**, 5084–5096.
44 S. M. Praveena, N. I. Shamsul Ariffin and A. L. Nafisyah, Microplastics in Malaysian bottled water brands: Occurrence and potential human exposure, *Environ. Pollut.*, 2022, **315**, 120494.
45 C. Chinglenthoiba, M. N. Lani, S. T. Anuar, K. T. T. Amesho, K. L. Priya and J. H. Santos, Microplastics in food packaging: Analytical methods, health risks, and sustainable alternatives, *J. Hazard. Mater. Adv.*, 2025, **18**, 100746.
46 J. Fu, N. Liu, Y. Peng, G. Wang, X. Wang, Q. Wang, M. Lv and L. Chen, An ultra-light sustainable sponge for elimination of microplastics and nanoplastics, *J. Hazard. Mater.*, 2023, **456**, 131685.
47 Y. Li, J. Fu, L. Peng, X. Sun, G. Wang, Y. Wang and L. Chen, A sustainable emulsion for separation and Raman identification of microplastics and nanoplastics, *Chem. Eng. J.*, 2023, **469**, 143992.

